Study of Formability of Brass Sheet Metal Under Different Temperature Conditions

V Dharma Singh[1*], *M Manzoor* Hussain [2] and *Swadesh Kumar* Singh [3]

[1]Mechanical Engineering Department, Muffakham Jah College of Engineering and Technology Hyderabad-500034, Telangana, India
[2] Mechanical Engineering Department, Jawaharlal Nehru Technological University Hyderabad-500085, Telangana, India
[3]Mechanical Engineering Department, GRIET, Hyderabad- 500090, Telangana, India

Abstract. In the present work focus devoted to the results obtained from uniaxial tensile test were utilized to analyze flow stress behavior of brass under different orientation, temperature and strain rate conditions and the study of forming limit diagrams for stretch forming of brass sheet material at room temperature and at various elevated temperatures have been estimated experimentally by performing stretch forming operations using warm forming tooling setup (i.e., suitable punch – die and blank holding set-up). After stretch forming the brass sheets metal at different temperature conditions (i.e., 300 K to 773 K) the minor and major strains are measured by using the electron microscope and then forming limit diagrams (FLDs) were constructed. With the help of forming limit diagram (FLDs) formability of brass analyzed. These formability limit diagrams (FLDs) were co-related with mechanical properties such as tensile strength and % elongation, and in-plane anisotropy of the brass sheet material.

1 Background

1.1 Introduction

Sheet Metal Forming is most important and essential manufacturing methods for producing the useful products in almost all industrial production, especially in the aircraft, automotive, food and home appliance industries. These methods are devoted to improve the formability, production of light weight and high strength complex-shaped parts with good surface quality, difficult to manufacture metals, reduce production cycle time of manufacturing. Ductility is an index of the formability which is the ability to deform a sheet metal plastically to achieve desired shape and size without causing any kind of failures. Formability of a sheet metal can be evaluated by knowing properties of material such as yield strength, tensile strength, percentage elongation, strain hardening exponent(n), strength coefficient (K), anisotropy

* Corrresponding author: dharamsingh10@gmail.com

coefficient etc. Stretching is one of sheet metal forming operation which is performed by suitable punch and die set-up. Stretchability of a sheet metal influences by various factors such as strain rate, strain-hardening exponent, strength coefficient, yield strength, tensile strength, ultimate strength, modulus of elasticity, etc. The test consists of clamping a test sample under controlled pressure between blank holder and die and then pressing the test sample into the die with the help of a hemi-spherical head punch, upto limiting value. Formability analysis is very important in manufacturing sector [1,2]. One of the most important technique to evaluate the formability of a sheet material is construction of forming limit diagram (FLD). It is most effective and powerful tool to estimate the limiting strains in different conditions. Sheet metal forming processes are widely applied in various industries to manufacture the components. In a sheet metal forming, a blank is stretched into a required shape by suitable tooling (i.e., Punch and die set-up) without any defects such as wrinkling or excessive thinning. In the past many year's techniques were developed to perform forming of high-strength material with low plasticity and difficult-to-form metals under cold, warm and hot forming conditions [3,4]. The important parameters related to mechanical properties of sheet material and improper consideration of this parameters in the design of sheet metal forming manufacturing processes leads to buckling, excessive thinning, tearing and wrinkling of the parts. Other parameters that influence the final shape of the parts include the geometry of the tool (i.e., punch-to-die clearance, die and punch radii) [5,6], friction conditions at the rubbing interface (i.e., dry or lubricated contact, lubricant type, contact pressure) [7–11], technological parameters (i.e., forming temperature, forming speed,) [12–14], tool material properties [15–17] and initial sheet metal surface topography [18–20]. The presence of frictional forces at the rubbing interface of tool and workpiece evaluates the nonuniformity of the sheet metal deformation and surface quality of the final component [21]. To predict the formability of sheet metal, various numerical models are widely employed in both industry and research.

Brass, a substitutional alloys of copper (Cu) and zinc (Zn) , is widely used for electric components, fasteners, ammunition components connections, and appliance parts due to its wide range of mechanical and electrical characteristics [22-24]. Brass is frequently replacement of copper in the production of fashion jewelry, costume jewelry, and other imitation jewelry. Brass alloy was also used to manufacture musical instruments like as bells and horns, as well as tiny gears [25]. As the Zn content increases in the Cu, its tensile strength and wear resistance increases upto 45 wt.% and upon exceeding 45 wt.% its strength deteriorated rapidly [26]. The most widely used brass in industrial applications consists of 30–45 wt.% Zn [27,28]. With addition of other alloying elements such as Al, Sn, Ni, Fe etc properties and performance can be enhanced [29,30]. Brass classified as α brass, α + β' brass, and β' brass, and their microconstituents and microstructures are changes with the content of Zn present. The strength and ductility of α brass are better than that of pure Cu at room temperature; β' brass is hard and less tough; α + β' brass stronger than α brass and tougher than β' brass, hence its applications are wider. Moreover, the high-temperature β phase is softer than the low-temperature β' phase, which results better hot workability of α + β' brass [31-34]. Electrical and thermal conductivity, durability, low melting point, easy formability and high strength after forming make this alloy desirable [4,7,8]. Despite its impressive formability, there are several severe drawbacks, such as a blackish tarnish or self-corrosion, which requires a lot of care. This non-destructive and natural self-corrosion is caused due to oxidization of the brass when exposed to air. The removal and prevention of tarnish is the most difficult aspect of brass maintenance. During stretch forming process, unpredicted failure reported much earlier than the expected failure either by forming limit diagrams or finite element simulations [9]. During the forming process, considerable amount of spring-

back observed and these are the main impediment for high-efficiency production in the industries.

Brass has relatively complex microstructures, resulting in typical plasticity [7,10–12]. The study emphasis has shifted to the deformation and failure features under room temperature and an extensive range of the strain rates for time and cost effective sheet metal production of brass components [10,12–15]. The majority of these studies found that strain hardening resulted in a rise in uniaxial tensile strength and a loss in flexibility. Elevated temperature testing is one of the most common ways to improve the ductility. elevated temperature testing softens the material which increases the formability of the part with reduced resistance to plastic deformation [16,17]. It also used to reduce the effect of spring-back. Second, selecting the right deformation parameter is critical for forming a complicated shape. The majority of the literature devoted on the impact of dynamic and intermediate strain rates [3,10,18–22]. However, there is still a disparity in mechanical characteristics under quasi-static strain rates, which is realistically connected to industrial forming of brass sheet. Padmavardhani and Prasad studied the strain rate and temperature effect on tensile flow behavior for β brass & α+β brass [21,22]. With a rise in temperature from 550ºC to 800ºC and a fall in 10^{2} to 10^{-3} s^{-1} strain rates, the flow stress and tensile strength were found to decreases.

After thorough literature review, it is found that no substantial studies have not presented on influence of the strain rates and test temperatures on overall mechanical and forming behavior of Commercially-Pure Brass. Thus, main objective of this research work is to understand mechanical and forming behavior of Commercially-Pure Brass tested between 0.001, 0.01 & 0.1 s^{-1} strain rates and temperatures (300 K, 573 K, 673 K and 773 K).

2 Materials and Methods

2.1 Material Composition

Optical Emission Spectroscopy with ASTM E478 used to determine the chemical composition of the parent brass sheet to evaluate raw materials and identify alloys. Elemental or composition analysis carried out can be qualitative (determining what elements are present), and quantitative (determining how much of each are present).

Table 1. Chemical composition of Brass sheet metal

Element	Zn	Pb	Fe	Cu	IMP
% in wt	Bal	0.292	0.1	64.305	0.6

2.2 Microstructure

Test sample was prepared as per the ASTM E3-95 standards. **Microscopic Examination** is conducted to study the microstructural features of the material under magnification and the microstructure consists of alpha and beta matrix.

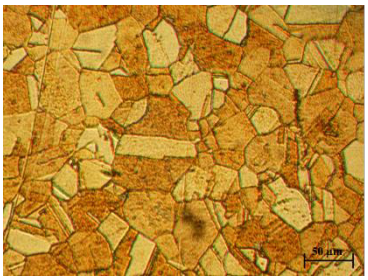

Fig. 1. Initial Microstructure of parent Brass sheet metal.

2.3 Hardness and Microhardness

Vickers hardness test with ASTM E92-17 was performed on the parent brass sheet and obtained the average hardness value of 78.3 HV5. Microhardness test performed by Vickers micro hardness tester with ASTM E384-16 on the parent brass sheet and obtained the average hardness value of 79.7 HV0.1.

3 Tensile Test

In the present study, commercially available Pure Brass was cold-rolled to 1 mm thickness and standard isothermal uniaxial tensile specimens were prepared as per the sub-sized ASTM E08/E8M-11, with help of wire cut EDM from cold rolled brass parent sheet with the gauge length of 30 mm, 21 mm width and 1 mm thickness, as depicted in Figure 2(a). Each specimen was polished by diamond pastes to remove scratches from the flat surface before conducting the test. In forming of brass sheet metal, mechanical properties and flow characteristics changes with respect to orientation because of inherent anisotropic nature. Thus, specimen were prepared by wire cut EDM at an angle of 0º, 45º, and 90º with respect to rolling direction, as depicted in Figure 2(b). Uniaxial isothermal tensile tests have been conducted at temperature of 300 K to 773 K under a constant quasi-static strain rates (0.001, 0.01 and $0.1s^{-1}$). The experiment was carried out on BISS Electra Servo Electric 50 KN loading capacity, computer controlled universal testing machine (UTM) under quasi-static straining condition. It is equipped with two zone split furnace, with a maximum 1000 ºC heating capacity with ± 3 °C accuracy, temperature of specimen was controlled through 3 thermocouples.

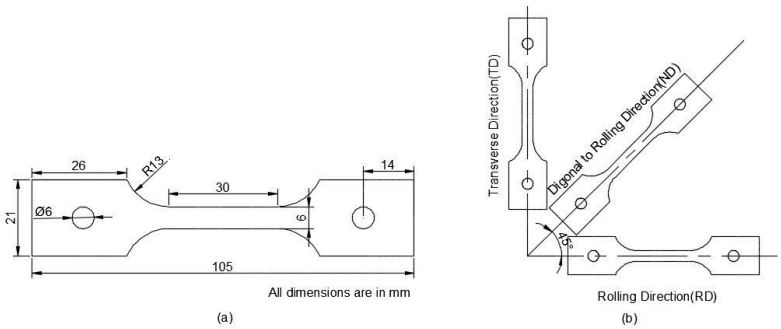

Fig. 2. Schematic of the (a) sub sized ASTM E08/E8M-11 standard test specimen and (b) different orientations of a sheet

Fig. 3. Uniaxial Tensile Test Machine

The influence of sheet orientation, test temperature and strain rate on flow stress behavior of brass have been analyzed. Figure 3 depicts the influence of test temperatures (300 K, 573 K, 673 K, and 773 K) on tensile flow behavior of brass for various strain rates. It is observed that with increase in test temperature significantly influence the yield stress/peak flow. The yield strength decreases with increase in the temperature. This is primarily because of softening phenomenon specifically at elevated temperature. This tendency is similar to most metals under uniaxial tensile deformation at the elevated temperature.

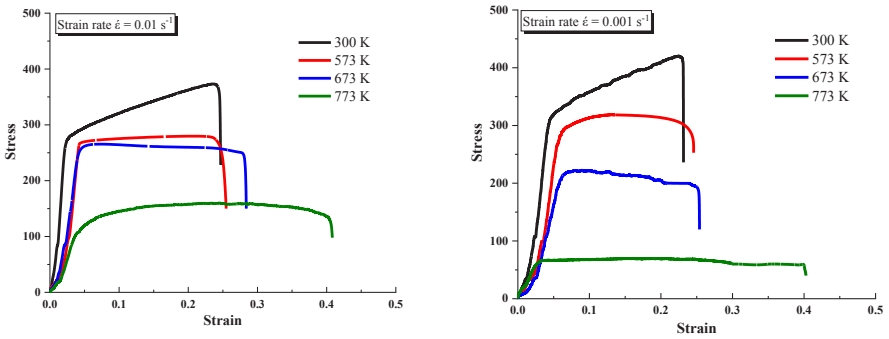

(a) (b)

Fig. 4. Influence of temperature on true stress-strain curves at (a) 0.01 s^{-1} and (b) 0.001 s^{-1}

The yield stress decreases mainly due to thermal activation of the dislocation motion which result in easier plastic deformation at elevated temperature [31]. Table 2 gives the calculated material properties of Brass. Figure 5 presents the influence of sheet orientation on flow stress behaviour at various test temperature at strain rate of 0.1/s. With change in sheet orientation minor influence noticed on yield stress but major influence on ultimate strength of the brass material. It is found that the tensile strength is superior along 0º orientation whereas drop in total elongation was noticed.

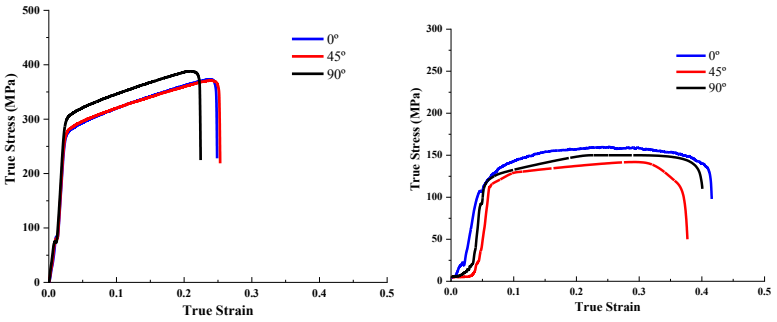

(a) (b)

Fig. 5. Influence of sheet orientation on flow stress behaviour at strain rate of 0.1/s and at (a) 300 K & (b) 773 K

Table 2. Average mechanical properties of brass sheet

Temperature	Orientation	YS (MPa)	UTS (MPa)	% elongation	In-plane Anisotropy (A_{IP})	Anisotropy index (δ)
300K	0°	305	404	30	0.07213	0.0909
	45°	290	380	29		
	90°	276	369	25		
573K	0°	293	354	36	0.07167	0.0746
	45°	271	341	32		
	90°	273	341	31		
673K	0°	184	202	39	0.07065	0.06849
	45°	175	198	35		
	90°	167	181	34		
773 K	0°	127	126	43	0.06693	0.0487
	45°	120	126	39		
	90°	117	123	36		

4 Nakazima Test

The most popular formability test Nakazima is utilized to predict the maps of the forming process. Therefore, the investigation of forming limits of Brass sheet was predicted using a stretch-forming tooling set-up with hemispherical punch (of ϕ50 mm), die, and blank holder is depicted in Figure 6. Induction heating system with a temperature controller with a K-type thermocouples utilized to heat specimens and die at prescribed temperature. The K-type thermocouples were installed at proper locations of punch and die set-up to measure test temperature. All stretching test were performed using molybdenum-based lubricant (Molykote). ASTM E2218-15 standard was utilized to prepare the different geometry and dimension blanks to plot forming limit diagrams (FLDs) [32]. Different geometry of specimens are presented in Figure 7(a) and stretch formed specimens are depicted in figure 7 (b). The draw bead was present in blank holder for holding the blank firmly without any slippage and to avoid easy flow of flat flange part into die cavity. To set the optimal process parameters, few trials were conducted initially and then stretch forming tests were performed

at different test temperatures (300 K to 773 K) with a constant punch velocity of 2 mm/min and blank holding pressure of 2.5 MPa.

For the measurement of major and minor strains, all specimens are laser-etched by 2.5 mm combined circular in square grid. Stretched specimens are differentiated by necking, safe, and fracture zones. Precise and accurate measurement of the deformed grid is one of the most critical issues to get accurate limiting strains in the FLD. Major and minor diameters of stretched grid (ellipses) in stretched blanks were measured with the help of an optical microscope to estimate engineering minor (e_2) and major (e_1) strains using Equation 1 & 2. Then transferred into corresponding true strains (ε_1 & ε_2) as in Equation 3.

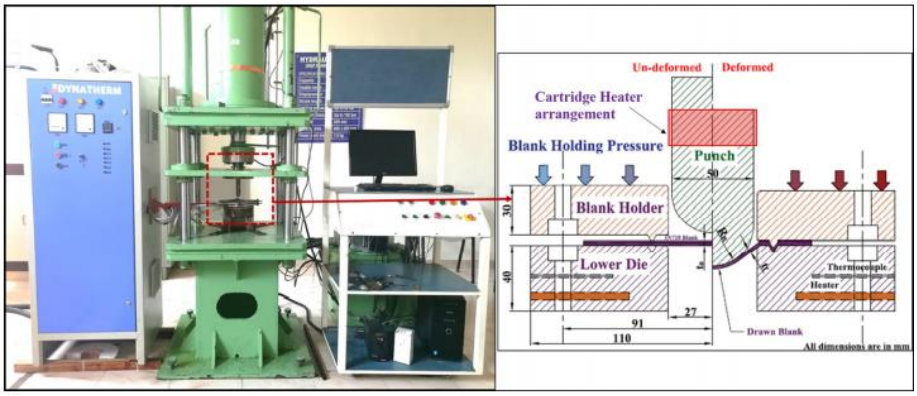

Fig. 6. 2D- schematic diagrams of stretch forming test setup for FLD and FFLD evaluation.

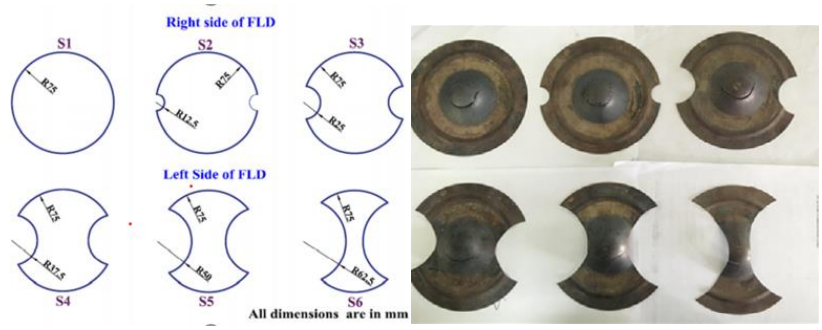

Fig. 7. (a). Specimen geometry studied for the FLDs plots & (b). Stretch formed specimens.

$$e_1 = \frac{\text{major axis of deformed ellipse} - \text{grid diameter}}{\text{major axis of the deformed ellipse}}, \quad (1)$$

$$e_2 = \frac{\text{minor axis of deformed ellipse} - \text{grid diameter}}{\text{minor axis of the deformed ellipse}} \quad (2)$$

$$\varepsilon_{1,2} = \ln(1 + e_{1,2}) \quad (3)$$

5 Analysis of Formability

5.1 Formability Limit Diagram (FLD)

The true major and minor strain at different temperature were estimated as plotted in Figure 8. These strains are differentiated by different symbols named as safe, necking and fracture strains. It is noticed that the considerable necking tendency have been reported before the failure of material. Solid symbols denotes the safe forming limit of the brass sheet metal. Forming limit curve (FLC) also known as a solid line, is drawn to distinguish the safe and failure strain regions. Three main deformation zones in FLD are biaxial tension, plane strain and tension-compression. It is noticed that the slope of FLC at 300 K changes from 0.63 to 0.05 in tension-compression and biaxial tension zones respectively. The slope of FLC in tension-compression zone is significantly influenced by the forming test temperatures. Whereas the slope of FLC in biaxial tension zone slightly decreases from 0.15 to 0.13 with increase in temperature. It is found that the forming limits were improved by 56 % with increase in forming test temperature from 300 K to 773 K. This conforms the forming test temperature plays an important role in FLD prediction.

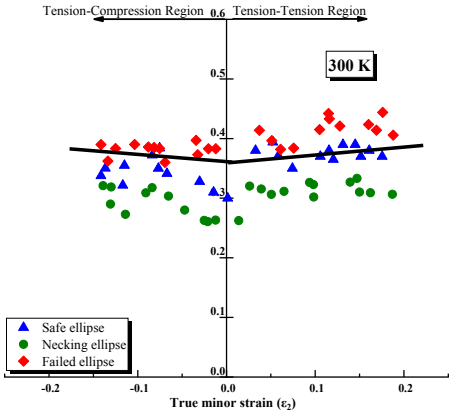

(a)

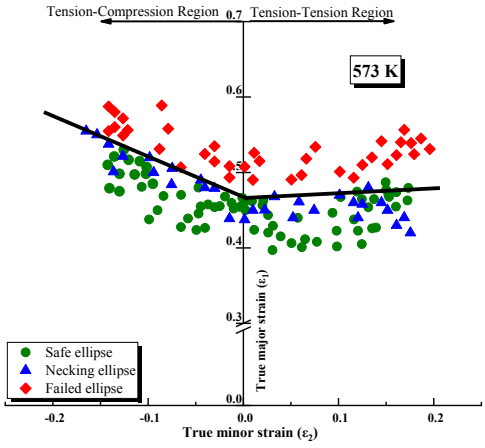

(b)

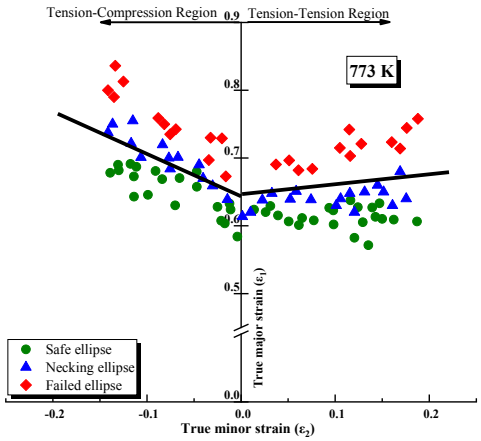

(c)

Fig.8. Experimental FLD at (a) 300 K (b) 573K (c) 773K

6 Conclusions

Following are the major conclusions made from the present study:

Tensile flow stress behaviors at elevated temperature condition have been influenced significantly by test temperatures and various strain rates for Brass. Decrease in yield and ultimate tensile strength have been noticed approximately 56 % and 65 % with increase in test temperature from 300 K to 773 K. Around 28% improvement has been noticed in % elongation with increase in test temperature.

Formability of Brass at four different forming temperatures (300K, 573 K, and 773 K) have been estimated by means of FLD and it is noticed that forming limits have improved by 53 % with increase in forming test temperature from 300 K to 773 K.

References

1. V Dharam Singh, Gauri Mahalle, Nitin Kotkunde, Swadesh Kumar Singh, M Manzoor Hussain, Advances In Materials and Processing Technologies, Taylor & Francis (**2021**).
2. Tomasz Trzepiecinski, Recent Developments and Trends in Sheet Metal Forming. Metals, 10, 779, **(2020)**
3. H. Hagenah, R. Schulte, M. Vogel, J.Hermann, H. Scharrer, M. Lechner, M. Merklein, Procedia CIRP, 79, 649–654 (**2019)**
4. Z. Gronostajski, Z. Pater, L. Madej, A. Gontarz, L. Lisiecki, A. Lukaszek-Solek, J. Luksza, S. Mróz, Z. Muskalski, W. Muzykiewicz, Arch. Civ. Mech. Eng., 19, 898–941(**2019)**.
5. S.S. Han, J. Mater. Process. Technol., 63, 129–133 (**1997)**.
6. P.Y.Wang, Z.J. Wang, N. Xiang, Z.X. Li, J. Manuf. Process., 53, 364–375 (**2020)**.
7. M.P Shisode, J. Hazrati, T. Mishra, M. de Rooij, Procedia Manuf., 47, 586–590 (**2020)**.
8. E. Evin, M. Tomáš, Mater. Sci. Forum, 994, 223–231(**2020)**.
9. H.B. Löfgren, Theory. Appl. Mech. Lett., 8, 57–61(**2018)**.

10. L. Figueiredo, A. Ramalho, M.C. Oliveira, L.F. Menezes, Wear, 271, 1651–1657 (**2011**).
11. W. Wang, Y. Zhao, Z. Wang, M. Hua, X. Wei, Tribol. Int., 93, 17–28 (**2016)**.
12. Z.Wang, R. Gu, S. Chen, W. Wang,X. Wei, J. Mater. Process. Technol., 257, 180–190 (**2018)**.
13. M. Kowalik, T. Trzepiecinski, Arch. Civ. Mech. Eng., 12, 292–298 (**2012)**.
14. K. Seshacharyulu, C. Bandhavi, B.B. Naik, S.S. Rao, S.K. Singh, Mater. Today Proc., 5, 18238–18244 (**2018)**.
15. J.Jaworski, T. Trzepieci ´ nski, Kov. Mater.Met. Mater., 54, 17–25 (**2016)**.
16. L. Kirkhorn, V. Bushlya, M. Andersson, J.E. Ståhl, Wear, 302, 1268–1278 (**2013)**.
17. M.H. Sulaiman, R. N. Farahana, K. Bienk, C.V. Nielsen, N. Bay, Wear, 438–439, 203040 (**2019)**.
18. C. Wang, R. Ma, J. Zhao, J. Zhao, J, J. Manuf. Process., 27, 126–137 (**2017)**.
19. F. Flegler, S. Neuhäuser, P. Groche, Tribol. Int., 141, 105956 (**2020)**.
20. A. Makhkamov, D. Wagre, A.M. Baptista, A.D. Santos, L. Malheiro, Ciência Tecnol. dos Mater., 29, e249–e253 (**2017)**.
21. M. Sigvant, J. Pilthammar, J. Hol, J.H. Wiebenga, T. Chezan, B.Cerleer, T. van den Boogard, Procedia Manuf., 29, 512–519 (**2019)**.
22. R.N.Wright, Ed.; 1st ed.; Elsevier, (**2016**).
23. D.D.Ratnayaka, M.J. Brandt, K.M. Johnson, *Water Supply*; 6th ed.; Elsevier, (**2009).**
24. W.S.Young, In *Encyclopedia of Materials: Science and Technology*; Elsevier, pp. 3645–3649 (**2001**).
25. K. Gupta, N.K. Jain, R. Laubscher, Advanced Gear Manufacturing and Finishing Classical and Modern Processes; Elsevier, (**2017**).
26. E.B. Zaretsky, G.I. Kanel, J. Appl. Phys., 124, 045902 (**2018**).
27. A. Davoodi, S. Honarbakhsh, G.A. Farzi, Prog. Org. Coat, 88, 106–115 **(2015**).
28. M. Adineh, H. Doostmohammadi, R. Raiszadeh, Iran. J.: Mater. Sci. Eng., 16, 21–32 **(2019)**.
29. S. Sohn, T. Kang, J. Alloy. Comp., 335, 281–289 (**2002**).
30. A.W. Bydalek, A. Kula, L. Blaz, K. Najman, Arch. Foundry Eng., 19, 21–26 **(2019**).
31. L. Suárez, P. Rodriguez-Calvillo, J.M. Cabrera, A. Martinez-Romay, D. Majuelos-Mallorquin, A. Coma, Mater. Sci. Eng. A, 627, 42–50 **(2015**).
32. C.A. Badrish, N. Kotkunde, G. Mahalle, S.K. Singh, K. Mahesh, *J. Mater. Eng. Perform.*, *28* (12), 7537–7553 (**2019)**.
33. ASTM E2218-15 Standard Test Method for Determining Forming Limit Curves. *ASTM B. Stand.*, 1–15 (**2015**).
34. G. Mahalle, A. Morchhale, N. Kotkunde, A.K. Gupta, Y.C. Lin, *J. Manuf. Process.*, *56*, 482–499 (**2020)**.